Science of the Total Environment 834 (2022) 155484

Contents lists available at ScienceDirect

Science of the Total Environment

journal homepage: www.elsevier.com/locate/scitotenv

Pyrolysis and combustion characteristics of typical waste thermal insulation materials

Wenlong Zhang [a], Jia Jia [b], Jiaqing Zhang [c], Yanming Ding [a,*], Juan Zhang [a], Kaihua Lu [a], Shaohua Mao [a]

[a] Faculty of Engineering, China University of Geosciences, Wuhan 430074, China
[b] Naval Research Institute, Beijing 100161, China
[c] Anhui Province Key Laboratory for Electric Fire and Safety Protection, State Grid Anhui Electric Power Research Institute, Hefei 230601, China

HIGHLIGHTS

- Pyrolysis and combustion are important methods to dispose of solid wastes.
- Pyrolysis and combustion characteristics of EPS and XPS are analyzed and compared.
- EPS has better pyrolysis properties, and XPS has better combustion characteristics.

GRAPHICAL ABSTRACT

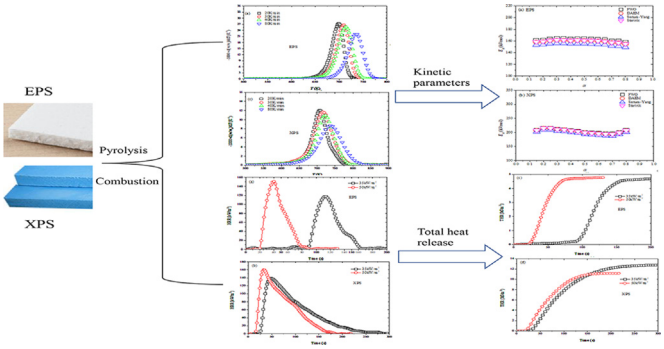

ARTICLE INFO

Editor: Huu Hao Ngo

Keywords:
Thermal insulation materials
Expanded polystyrene
Extruded polystyrene
Pyrolysis properties
Combustion characteristics

ABSTRACT

Thermal insulation materials are important for building energy conservation, but their wastes have increased sharply. Furthermore, pyrolysis and combustion are increasingly utilized to dispose of solid wastes and convert them into value-added fuels. To better understand the pyrolysis and combustion characteristics of these materials, typical thermal insulation materials (expanded polystyrene (EPS) and extruded polystyrene (XPS)) were investigated by employing thermogravimetry and differential scanning calorimetry as well as cone calorimetry experiments. Pyrolysis behavior, kinetic parameters, pyrolysis index, thermodynamic parameters, endothermic properties and combustion parameters were estimated comprehensively. The results showed that EPS had better pyrolysis properties, while XPS had better combustion characteristics. Activation energies of EPS and XPS were 158.82 kJ/mol and 200.70 kJ/mol, respectively. Additionally, EPS had a higher pyrolysis stability index and comprehensive pyrolysis index, meaning a more intense reaction. Moreover, thermodynamic parameters indicated that the devolatilization products could be obtained easily from the two materials, and EPS and XPS could be converted into fuels. For the combustion, XPS had a smaller fire performance index and a larger fire growth index. These results can guide the reactor design and optimization for better converting polymer wastes into fuels and managing wastes.

1. Introduction

Energy consumption is a significant issue for the sustainable development of all countries in the world. In this case, the energy consumption of buildings accounts for about 40% of global energy, so it is a necessity for reducing building energy consumption (Masri et al., 2018). To achieve this goal, there are many studies on measures for the efficient energy utilization of buildings, particularly the use of thermal insulation materials is extensively acknowledged. As a typical thermal insulation material, polystyrene (PS) has many superior advantages, such as light weight, low cost and excellent mechanical properties. It is commonly used as the core material of external thermal insulation systems to reduce energy consumption (Zhang et al., 2021).

* Corresponding author.
E-mail address: dingym@cug.edu.cn (Y. Ding).

http://dx.doi.org/10.1016/j.scitotenv.2022.155484
Received 26 February 2022; Received in revised form 17 April 2022; Accepted 19 April 2022
Available online 23 April 2022

Since these thermal insulation materials have intrinsic flammability, some researchers suggest replacing the combustible thermal insulation materials currently installed with non-combustible materials, which will generate a large number of wastes. In addition, in the current use, refurbishment of the building has resulted in numerous quantities of wastes (Ni et al., 2020). However, these wastes are intractable and not biodegradable (Chauhan et al., 2008), so the accumulation of wastes will cause environmental issues (Yu et al., 2019) and even pose a threat to the public health (Nisar et al., 2019). Therefore, the management and recycling of waste thermal insulation materials is an urgent task. In general, landfills (Mangesh et al., 2020), pyrolysis (Ding et al., 2020b) and combustion (Qi et al., 2021) are mostly chosen to manage solid wastes. Therein, landfills have obvious environmental threats because of landfill gas and leachate (Siddiqui et al., 2019). Different from landfills, pyrolysis and combustion can give various energy products, including gas fuel, liquid fuel, et al. (Ding et al., 2020a), which are expected to play a more important role in the management of solid wastes and conversion into alternative fuels (Ding et al., 2021). For example, Li et al. (2019) handled waste rigid polyurethane with pyrolysis. Chen et al. (2019a) used combustion to deal with thermo-setting plastic wastes and acquired flammable gas.

In previous literature, many studies were conducted to dispose of waste PS and obtain products by using pyrolysis. Chauhan et al. (2008) noted that valuable hydrocarbon fuels could be acquired from PS waste by pyrolysis. Kumar and Singh (2013) found that PS could be degraded into a lot of monomers, which was the main product of pyrolysis. Faravelli et al. (2001) introduced a detailed model to describe the reaction process of PS, so as to convert the waste into energy-dense material. As commonly used PS, expanded polystyrene (EPS) and extruded polystyrene (XPS) are widely utilized, but their pyrolysis and combustion characteristics are different because of the different production processes. Jiao et al. (2012) obtained the activation energy of EPS and XPS, and their results showed that the activation energy of EPS was in the range of 220–230 kJ/mol, which was lower than 245 kJ/mol of XPS. Ni et al. (2020) determined the reaction mechanism of EPS, and the reaction function was $g(\alpha) = 1 - (1 - \alpha)^3$. Jiang et al. (2018) estimated the reaction mechanism of XPS, which was $g(\alpha) = -\ln(1 - \alpha)$. Significantly, EPS and XPS have different kinetic parameters and reaction mechanisms. However, these different parameters and mechanisms are imperative for modeling the reactor (Zhang et al., 2022), so understanding the difference between EPS and XPS is conducive to designing suitable reactors for managing and recycling these wastes.

Apart from pyrolysis, researchers also focus on the combustion performances of PS. Wang et al. (2018) studied the fire performance of EPS with the cone calorimeter test. An et al. (2015) conducted the correlation analysis of heat flux and thickness for PS based on the cone calorimetry test data. These valuable results can provide a good understanding of the combustion properties of this type of polymer. Nevertheless, the comparisons of the combustion characteristics of EPS and XPS are rare.

Although researchers have investigated the pyrolysis of EPS and XPS, they generally pay attention to the activation energy or reaction mechanism of a single material. Nevertheless, these common parameters, such as activation energy and reaction mechanism, are not sufficient to reflect the characteristics of pyrolysis. More in-depth information on the pyrolysis and combustion characteristics of the two materials has not been studied and compared in detail. To improve the efficiency of commercial pyrolyzers, detailed pyrolysis parameters are necessary (Khiari et al., 2019). In the current study, thermogravimetry, differential scanning calorimetry and cone calorimetry experiments were performed. Then, the kinetic parameters of EPS and XPS were calculated through multiple isoconversional methods, including Flynn-Wall-Ozawa, distributed activation energy model, Starink and Senum-Yang methods. Meanwhile, pyrolysis index and thermodynamic analysis were estimated based on the kinetics. Subsequently, the endothermic properties and the combustion characteristics of EPS and XPS were compared.

2. Material and methods

2.1. Materials

EPS and XPS are both produced by Shanghai Yubalong rubber insulation material Co. Ltd., Shanghai, China. These materials are composed of about 98% air and 2% polymerizing styrene, and the porosity between honeycombs of EPS and XPS are 98% and 96.5% (An et al., 2015), respectively. Their molecular formula is $(C_8H_8)_n$. Moreover, EPS and XPS, as typical thermoplastics, are greatly affected when heated. Before the tests, the samples were dried at 80 °C for 24 h and ground into powder.

2.2. Thermogravimetry and differential scanning calorimetry experiments

The samples were analyzed by the thermogravimetry and differential scanning calorimetry experiments, which were performed on a thermal analyzer (TA Instrument SDT Q600). 6 mg samples were heated from 300 K to 1000 K in nitrogen, and the heating rates were 20, 30, 40 and 80 K/min, respectively. Furthermore, the flow rate of gas was 100 mL/min.

2.3. Cone calorimetry

Combustion characteristics of EPS and XPS were measured by using a cone calorimeter device established by Fire Testing Technology. During the measurement process, samples of 100 mm × 100 mm × 20 mm were prepared, and their bottom and sides were wrapped with aluminum foil and a ceramic fiber blanket to maintain insulation. The samples were positioned horizontally, and the distance between the samples and the cone heater was 25 mm, which was exposed to two heat fluxes of 35 and 50 kW/m^2 according to ISO 5660-1 (2002).

2.4. Kinetic analysis

Thermogravimetric analysis (TGA), as a thermal analysis technique, can be conveniently and rapidly utilized to understand the pyrolysis process of solid (Li et al., 2020b).

Based on the thermogravimetric analysis, the kinetic equation can be characterized as:

$$\frac{d\alpha}{dT} = \frac{A}{\beta} f(\alpha) \exp\left(\frac{-E_\alpha}{RT}\right) \tag{1}$$

$$\alpha = \frac{m_0 - m_t}{m_0 - m_f} \tag{2}$$

where $d\alpha/dT$ is the reaction rate, α denotes the conversion rate, and T represents the temperature. A is the pre-exponential factor, and β is the heating rate. As for $f(\alpha)$, it means the differential form of integral function $g(\alpha)$ corresponding to the kinetic model. E_α is the activation energy, and R stands for the universal gas. Besides, three masses are called initial mass, intermediate mass and final mass for m_0, m_t and m_f, respectively.

There are many methods to estimate the kinetic parameters of pyrolysis. Especially, integral isoconversion methods have wide applications.

2.4.1. Flynn-Wall-Ozawa (FWO) method

The FWO method (Flynn and Wall, 1966) is a common isoconversion method to calculate the kinetics of solid thermal degradation (Ding et al., 2016), and the expression can be written as:

$$\ln\beta = \ln\left(\frac{AE_\alpha}{Rg(\alpha)}\right) - 5.331 - 1.052\left(\frac{E_\alpha}{RT}\right) \tag{3}$$

There is a linear relationship between heating rates and temperature ($\ln\beta$ versus $1/T$), and the slope can be used to estimate the E_α.

2.4.2. Distributed activation energy model (DAEM) method

Similar to the FWO method, the DAEM method (Miura, 1995) is also a linear method that can estimate the kinetic parameters. The simplification function gives:

$$\ln\left(\frac{\beta}{T^2}\right) = \ln\left(\frac{AR}{E_\alpha}\right) + 0.6075 - \frac{E_\alpha}{RT} \tag{4}$$

The E_α can be obtained from a slope of a straight line when plotting the $\ln(\beta/T^2)$ versus $1/T$.

2.4.3. Starink method

The Starink (Starink, 2003) method is the same as other integral isoconversion methods (such as FWO, DAEM) in calculating the kinetics, which can be expressed as Eq. (5).

$$\ln\left(\frac{\beta}{T^{1.92}}\right) = \ln\left(\frac{AE_\alpha}{Rg(\alpha)}\right) - 0.312 - 1.0008\left(\frac{E_\alpha}{RT}\right) \tag{5}$$

The left side of Eq. (5) and $1/T$ can give a line, whose slope can obtain the E_α.

2.4.4. Senum-Yang method

The Senum-Yang method (Senum and Yang, 1977) can be presented as Eq. (6), and the E_α is calculated from the plot of $\ln(\beta/T^2h(y))$ versus $1/T$.

$$\ln\left[\frac{\beta}{T^2h(y)}\right] = \ln\left(\frac{AE_\alpha}{Rg(\alpha)}\right) - \frac{E_\alpha}{RT} \tag{6}$$

where $y = E_\alpha/RT$, and the $h(y)$ can be shown as

$$h(y) = \frac{y^3 + 18y^2 + 88y + 96}{y^4 + 20y^3 + 120y^2 + 240y + 120} \tag{7}$$

Different from other isoconversion methods, the Senum-Yang method needs an iterative procedure when calculating the kinetic parameters. The detailed iterative procedure can be seen in Reference (Chen et al., 2019b).

2.5. Pyrolysis characteristic parameters

2.5.1. Pyrolysis index

Comprehensive pyrolysis index (D) means the reaction degree during thermal degradation, which has better pyrolysis performance with a higher value (Wang et al., 2020). The expression can be written as follows

$$D = \frac{(-R_P)(-R_V)M_f}{T_i T_p \Delta T_{1/2}} \tag{8}$$

where R_P and R_V are the maximum and average values of mass loss rate, and M_f means the residual mass. T_i is the initial temperature, which is obtained by the tangent method. T_p represents the temperature corresponding to the R_P. $\Delta T_{1/2}$ stands for the temperature range of half-peak width.

Besides, the pyrolysis stability index (R_w) (Shahbeig and Nosrati, 2020) denotes the stability of thermal degradation, which can be written as

$$R_w = 8.5875 \times 10^7 \times \frac{(-R_p)}{T_i \cdot T_p} \tag{9}$$

2.5.2. Thermodynamic parameters

In addition to the pyrolysis index, thermodynamic parameters can be employed to understand the pyrolysis characteristics (Niu et al., 2018).

$$\Delta H = E_\alpha - RT \tag{10}$$

$$\Delta G = E_\alpha + RT_P \ln\left(\frac{k_B T_P}{hA}\right) \tag{11}$$

$$\Delta S = \frac{\Delta H - \Delta G}{T_P} \tag{12}$$

ΔH is the apparent enthalpy change, ΔG represents apparent Gibbs free energy change, and ΔS means the apparent entropy change. k_B and h are the constants called Boltzmann constant (k_B, 1.381×10^{-23} J/K) and Plank constant (h, 6.626×10^{-34} Js).

3. Results and discussion

3.1. Thermogravimetric analysis

The derivative thermogravimetry (DTG) and thermogravimetry (TG) curves are shown in Fig. 1. EPS and XPS have a similar tendency at different heating rates, which indicates that the higher heating rate is the reason for the thermal degradation to move to a higher temperature. Although the reaction temperature is increasing with heating rates, the peak values of DTG curves are decreasing. The reason for this phenomenon is that the thermal conductivity of EPS and XPS is low, which is 0.029–0.041 W m^{-1} k^{-1} and 0.025–0.035 W m^{-1} k^{-1} (Stec and Hull, 2011), respectively. The heat exchange is insufficient from the sample surfaces to the inside when the sample is pyrolyzed at a high heating rate. In addition, the main pyrolysis range is 550–825 K.

Significantly, there are some differences between the EPS and XPS. Fig. 1 (a) shows that the initial mass loss temperature of EPS is about 625–675 K, and the final temperature is in the range of 725–775 K. Different from EPS, the DTG curves of XPS start from 550 to 600 K and end at 775–825 K, which is illustrated in Fig. 1 (c). The main reaction range of EPS is lower than that of XPS, which are 100 K and 225 K, respectively. Jun et al. (2006) and Jiao and Sun (2014) analyzed the pyrolysis of EPS and XPS, and the pyrolysis range was about 573–773 K and 573–823 K, which was close to the range of this study. Fig. 1 (b) and (d) is the TG curve of two materials, indicating that EPS has fewer residues. From the DTG and TG analyses, it is demonstrated that EPS has a high mass loss rate during pyrolysis, and more matrixes are involved in the pyrolysis reaction. The reason for the different pyrolysis behavior of EPS and XPS is that the differences in characteristics between the two materials exist, such as molecular weight, additives (Faravelli et al., 2001), heat transfer limitations and production processes (Xu et al., 2018).

3.2. Kinetic analysis

Activation energy is an imperative parameter for analyzing pyrolysis. It reflects the needed energy in the pyrolysis reaction, which can be used to evaluate the difficulty of further reaction (Liu et al., 2019).

As exhibited in Fig. 2, it displays that the average E_α of the two materials is 158.82 kJ/mol and 200.70 kJ/mol, respectively. Additionally, if the E_α keeps stable during the pyrolysis, it can be seen as a single-step reaction (Jiao et al., 2012). For example, Vyazovkin et al. (2020) suggested a range to judge whether the variation in E_α was significant, namely the ratio of the difference between the maximum and minimum value of E_α to the average E_α value was less than 10–20%. If the variation in E_α is less than 10–20% of the average value, E_α is independent of α, which can be considered to be stable. The values of the ratio of EPS are 11.13%, 12.13%, 4.46% and 4.22% for the four methods, while the ratio values of XPS are 9.59%, 10.48%, 10.92% and 12.62% for XPS, so EPS and XPS are single-step reactions.

Additionally, the comparison of the E_α of EPS and XPS between this study and the literature is listed in Table 1. It indicates that the E_α of the two materials is near that of the literature.

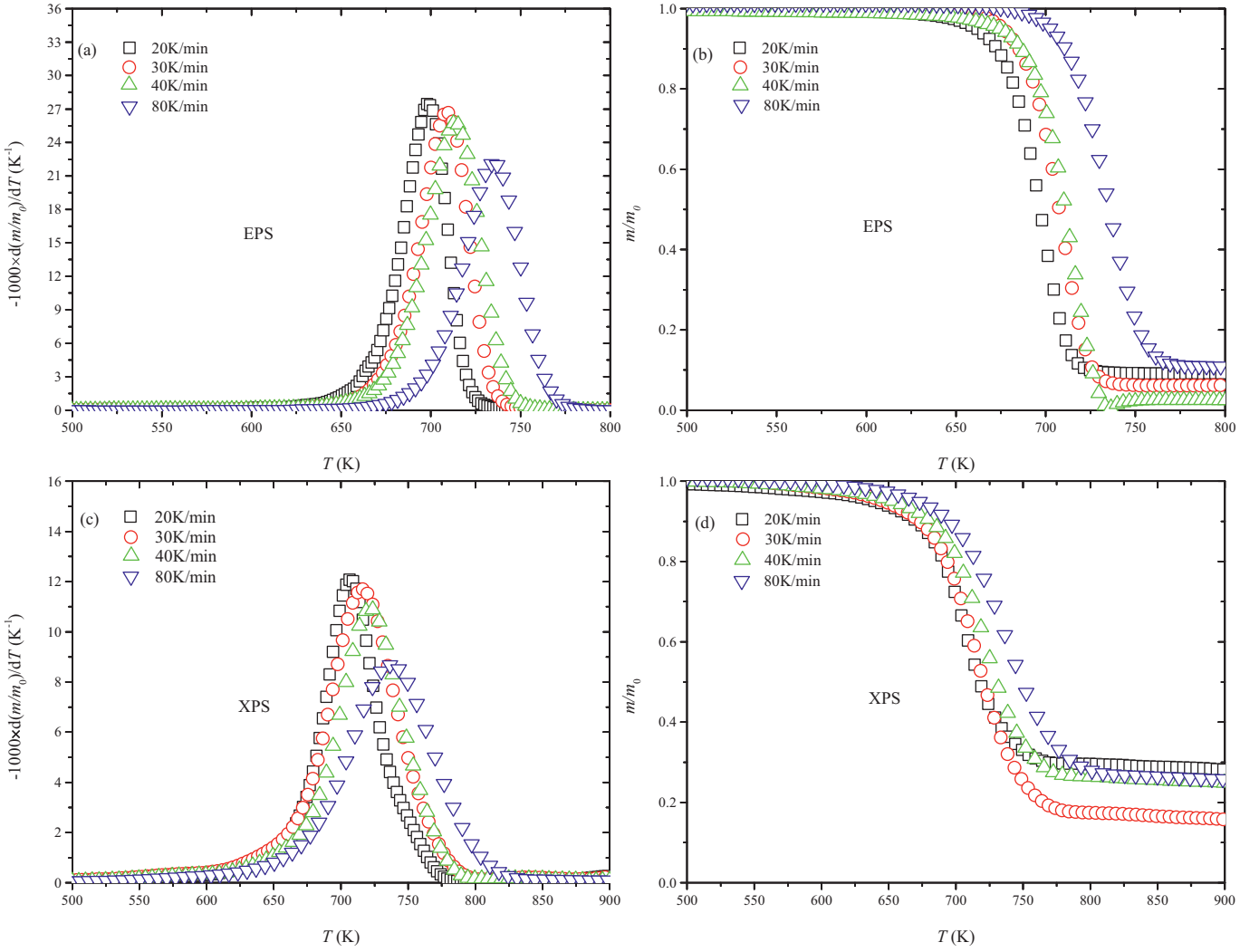

Fig. 1. Mass loss and DTG curves of EPS and XPS.

3.3. Pyrolysis index analysis

The pyrolysis index of EPS and XPS can be calculated based on the parameters of the DTG and TG curves, such as T_i, T_e and T_p. These parameters are demonstrated in Fig. 3.

The detailed parameters and calculated pyrolysis index are presented in Table 2. From Table 2, it appears that temperatures are related to the heating rates, and three temperatures (T_i, T_e and T_P) increase with the heating rates. For XPS, T_i is lower than that of EPS at multiple heating rates, while T_e is larger. Moreover, the R_w of XPS is lower, indicating that

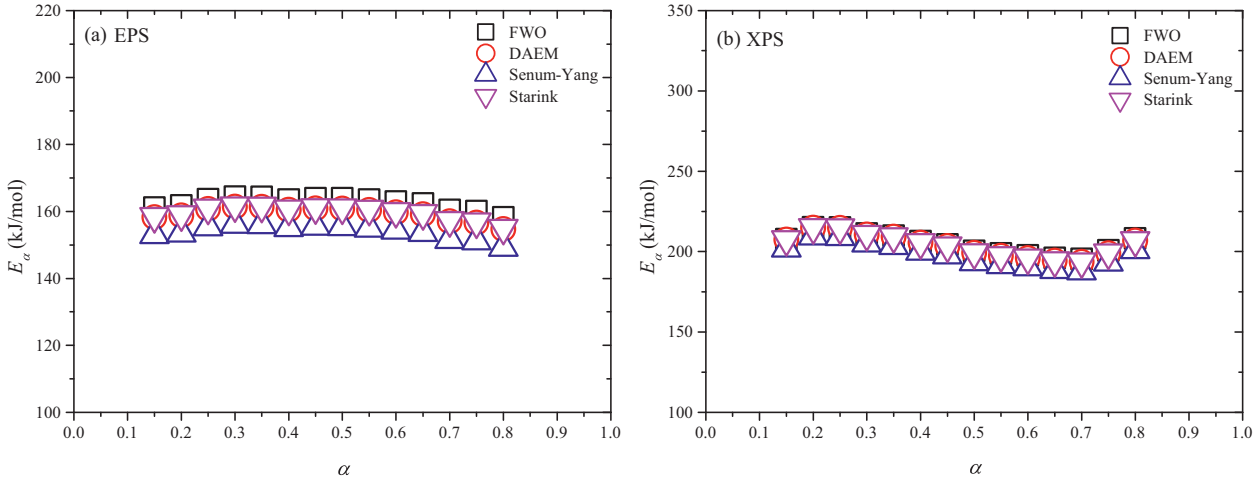

Fig. 2. The E_α of EPS and XPS.

Table 1
The comparison of the E_α of EPS and XPS between this study and the literature.

Materials		Calculation values	Jun et al. (2006)	Jiao et al. (2012)	Ni et al. (2020)	Li et al. (2020a)
EPS	Range	149–214	140–179	–	154–166	–
	Average	158.82	153.48	245	163.23	–
XPS	Range	183–215	–	220–230	–	177–212
	Average	200.70	–	–	–	200.43

XPS has an unstable state during the pyrolysis compared with EPS. What is more, the higher value of D suggests that EPS has better pyrolysis properties than XPS.

3.4. Thermodynamic parameters analysis

The thermodynamic parameters of the two materials are calculated by using the FWO method, and the calculated values are depicted in Fig. 4. The ΔH indicates the total energy needed to convert into products during the pyrolysis process, and it also reflects the presence of endothermic reactions during the pyrolysis when the value is positive (Shahbeig and Nosrati, 2020). Fig. 4 (a) shows that the pyrolysis of EPS and XPS is endothermic, and similar results can be verified by differential scanning calorimetry (DSC) analysis in Section 3.5. Moreover, the ΔH of XPS is larger than that of EPS, so XPS needs more energy, which is the same as the results of E_α. Additionally, potential barriers (E_α-ΔH) are small for pyrolysis of EPS and XPS, and they are 5.69–5.93 kJ/mol and 5.63–6.11 kJ/mol, respectively. The small difference in potential barriers means that the devolatilization products can be obtained easily from the two thermal insulation materials.

The ΔG illustrates the amount of available energy obtained from pyrolysis (Mehmood et al., 2019), which indicates the energy potential through the conversion of pyrolysis. The calculated value of ΔG shows that EPS and XPS can be converted into energy products. The ΔG of EPS decreases from 0.15 to 0.30 of α, then it increases. Unlike EPS, the ΔG of XPS increases in the initial reaction stage (0.15–0.30). Sahoo et al. (2020) noted that the provided heat energy to the system would not be released immediately if the ΔG decreases as α increases. Consequently, at the initial reaction stage, the heat energy of XPS is released rapidly.

The ΔS shows the disorder degree in the pyrolysis process. Negative values of ΔS indicate that products are more organized, and a thermodynamic equilibrium can be achieved (Shahid et al., 2019). In addition, the ΔS values of EPS and XPS are stable, exhibiting that the pyrolysis reaction is simple (single-step reaction) (Mehmood et al., 2019), which has a similar conclusion in Section 3.2.

3.5. Differential scanning calorimetry analysis

The DSC curves are exhibited in Fig. 5. It shows that EPS has one endothermic peak, so pyrolysis of EPS can be deemed as a typical depolymerization mechanism (Peterson et al., 2001). The corresponding temperature range of the endothermic peak is 675–740 K, which is close to 673–723 K obtained by Jiao et al. (2012). Compared with EPS, there are two endothermic peaks for XPS with a temperature range of 425–500 K and 675–750 K. Jiao et al. (2012) noted that the DSC curve of XPS showed a small peak in the range of 501 K and 571 K, but it was inapparent in their paper. Different from the above literature, the current study displays an obvious endothermic peak near 500 K.

There is one more endothermic peak of XPS than EPS, which means that XPS needs more energy to support continued pyrolysis. The reason for different DSC characteristics may be that XPS begins to react at the initial thermal degradation stage, and thermal scission happens at weak link sites in the current stage (Peterson et al., 2001). As for the different endothermic peaks of the two materials, it may be explained by the differences in characteristics (Faravelli et al., 2001).

3.6. Cone calorimetric analysis

The cone calorimetry, as an important bench scale instrument, is widely used to test combustion characteristics (Zhao et al., 2017). Besides, the corresponding data are significant parameters for analyzing the material's flammability, such as heat release rate (HRR) and total heat release (THR) and so on. The HRR and THR of EPS and XPS under heat fluxes of 35 and 50 kW/m^2 are shown in Fig. 6. With the increase of heat flux, the time to ignition (TTI) becomes earlier, while the peak value of HRR (PHHR) is larger. As for THR, it keeps stable under different heating fluxes.

The fire performance index (FPI) is a parameter that indicates the fire hazard of material, and it is obtained by the ratio of TTI to PHRR (Zhao et al., 2017). Moreover, the higher the FPI value of the material is, the lower the risk of fire is. Apart from FPI, the fire growth index (FGI = PHRR/TPHRR, TPHRR is the time when the peak of HRR occurs) is also an important index to evaluate the flammability characteristics, and the material will have a low fire hazard if the FGI value is small. The parameters of cone calorimetry are listed in Table 3.

Table 3 shows that the TTI of EPS is 87 and 19 s, while it is 24 and 15 s for XPS. Since TTI is an important parameter for evaluating the flammability characteristics of materials (Jian et al., 2014), it indicates that XPS is

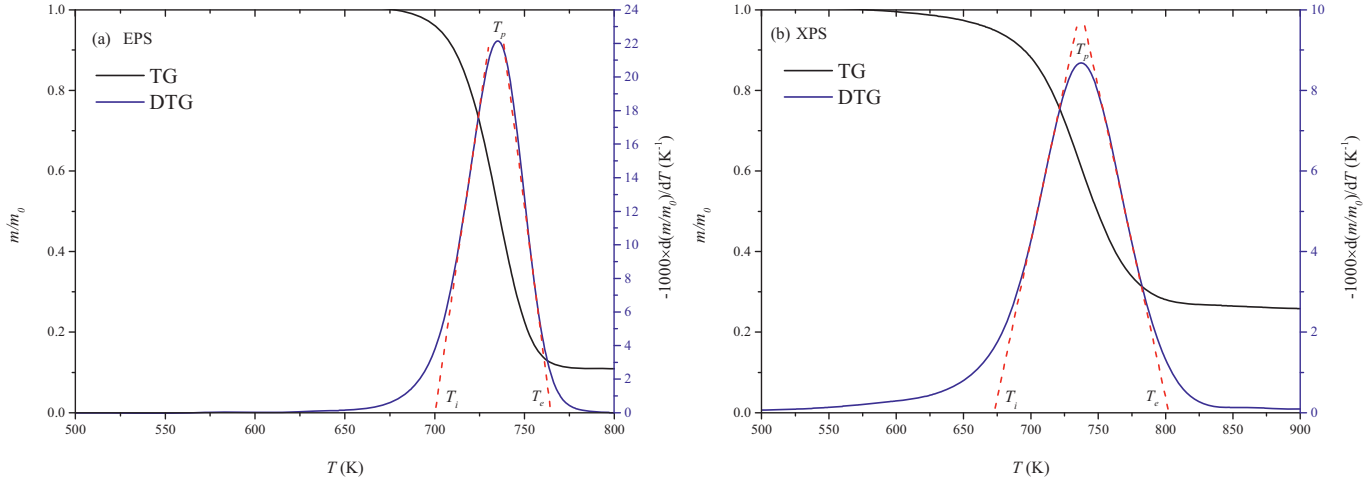

Fig. 3. The parameters from a scheme of DTG and TG curves at 80 K/min.

Table 2
The pyrolysis index of EPS and XPS.

Materials	β (K/min)	T_i (K)	T_e(K)	T_p (K)	R_p ($10^{-3}K^{-1}$)	R_v (10^{-3} K^{-1})	M_f	R_w ($10^{-3}K^{-3}$)	D (10^{-13} K^{-5})
EPS	20	668.66	718.70	698.49	27.50	16.24	0.10	5.06	35.29
	30	680.55	730.22	710.07	28.03	17.11	0.08	4.98	27.52
	40	683.58	737.11	714.90	28.74	17.22	0.02	5.05	7.09
	80	700.57	764.77	735.10	22.15	12.95	0.12	3.69	18.58
XPS	20	664.91	746.84	707.11	12.08	5.76	0.34	2.21	11.22
	30	663.54	770.33	715.91	11.69	6.80	0.18	2.11	5.19
	40	671.91	772.18	721.60	10.92	5.79	0.28	1.93	6.42
	80	673.27	802.01	737.22	8.68	5.14	0.28	1.50	3.40

more flammable than EPS. The combustion time of XPS is longer, so XPS can bure more time in the fire. Moreover, the THR of XPS is noticeably larger than that of EPS, which shows that XPS can release a large amount of heat during combustion. Furthermore, the FPI value of XPS is lower than that of EPS, while the FGI value is larger at 35 and 50 kW/m^2, indicating that XPS has better combustion characteristics.

4. Conclusions

To effectively recycle and convert the representative thermal insulation materials into fuels by using the pyrolysis and combustion technique, pyrolysis and combustion characteristics of thermal insulation materials were studied. A series of thermogravimetry, differential scanning calorimetry and cone calorimetry experiments were performed. Furthermore, the kinetic parameters of EPS and XPS were calculated by using multiple kinetic methods, including the Flynn-Wall-Ozawa, distributed activation energy model, Starink and Senum-Yang methods. Pyrolysis index and thermodynamic parameters were evaluated based on the thermogravimetric data. Subsequently, the endothermic reactions were determined, and the combustion characteristics were analyzed. The results showed that EPS had better pyrolysis properties, while XPS had better combustion characteristics. Both EPS and XPS had potential as energy sources. Thus, it is beneficial to reactor design and optimization according to the different properties of the two materials.

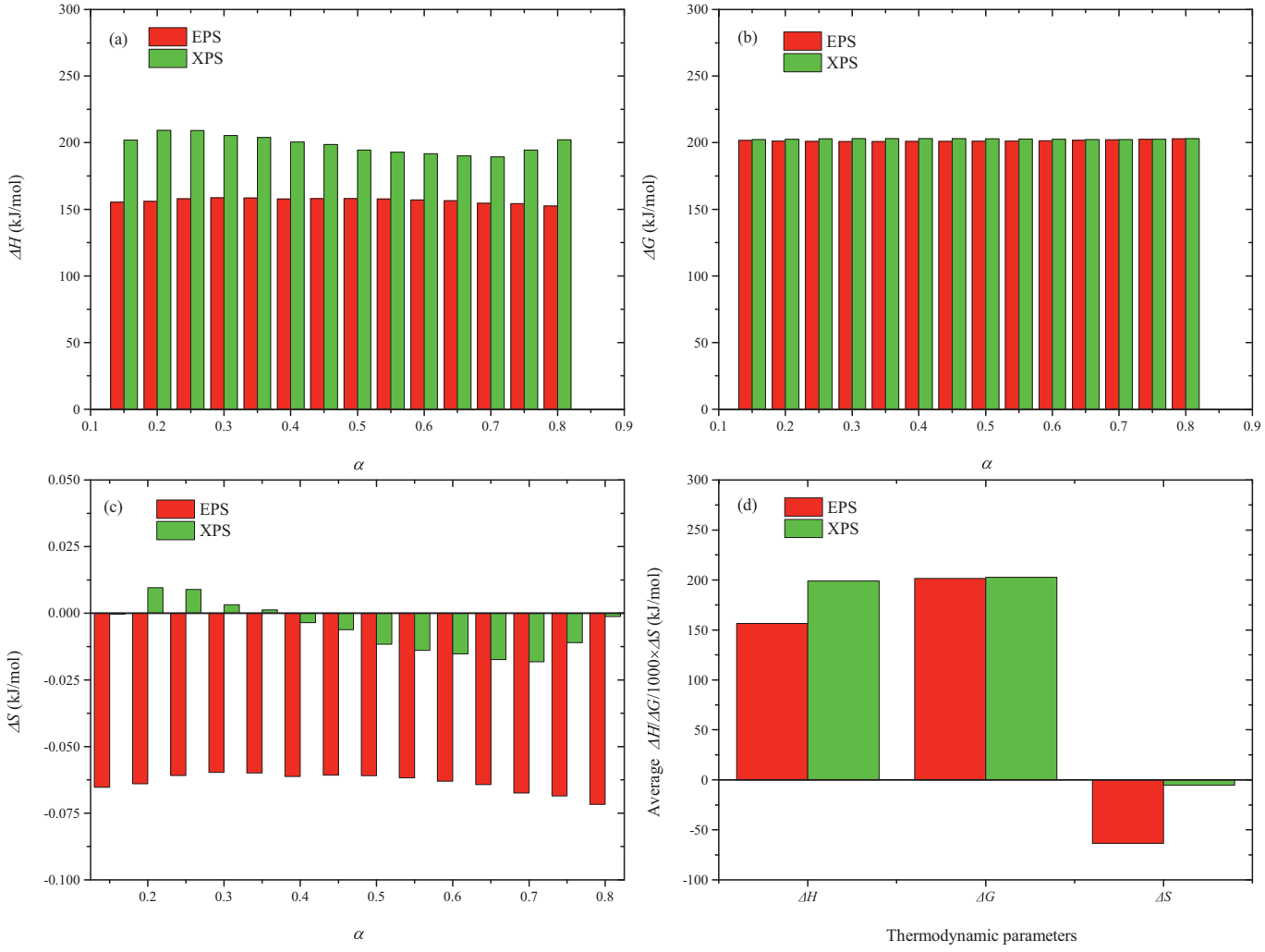

Fig. 4. The calculated thermodynamic parameters of the two materials by the FWO method.

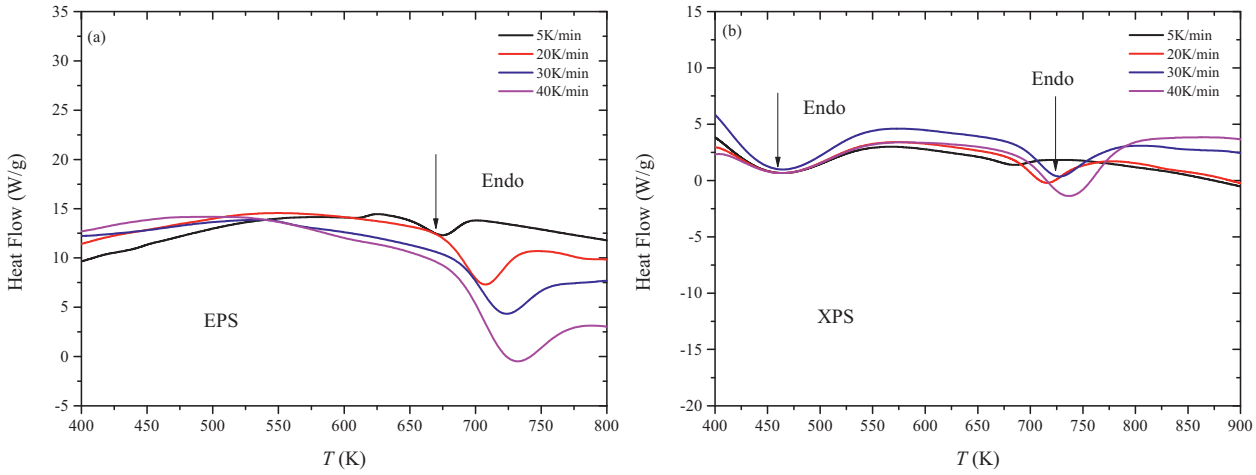

Fig. 5. The DSC curves of EPS and XPS.

CRediT authorship contribution statement

Wenlong Zhang: Conceptualization, Writing - original draft, Writing - review & editing, Investigation, Visualisation. **Jia Jia:** Formal analysis, Writing - review & editing. **Jiaqing Zhang:** Data curation, Writing - review & editing. **Yanming Ding:** Conceptualization, Methodology, Validation, Writing - original draft, Writing - review & editing, Visualisation. **Juan Zhang:** Data curation, Writing - original draft, Writing - review & editing. **Kaihua Lu:** Methodology, Software, Writing - original draft, Writing - review & editing. **Shaohua Mao:** Conceptualization, Writing - original draft, Writing - review & editing.

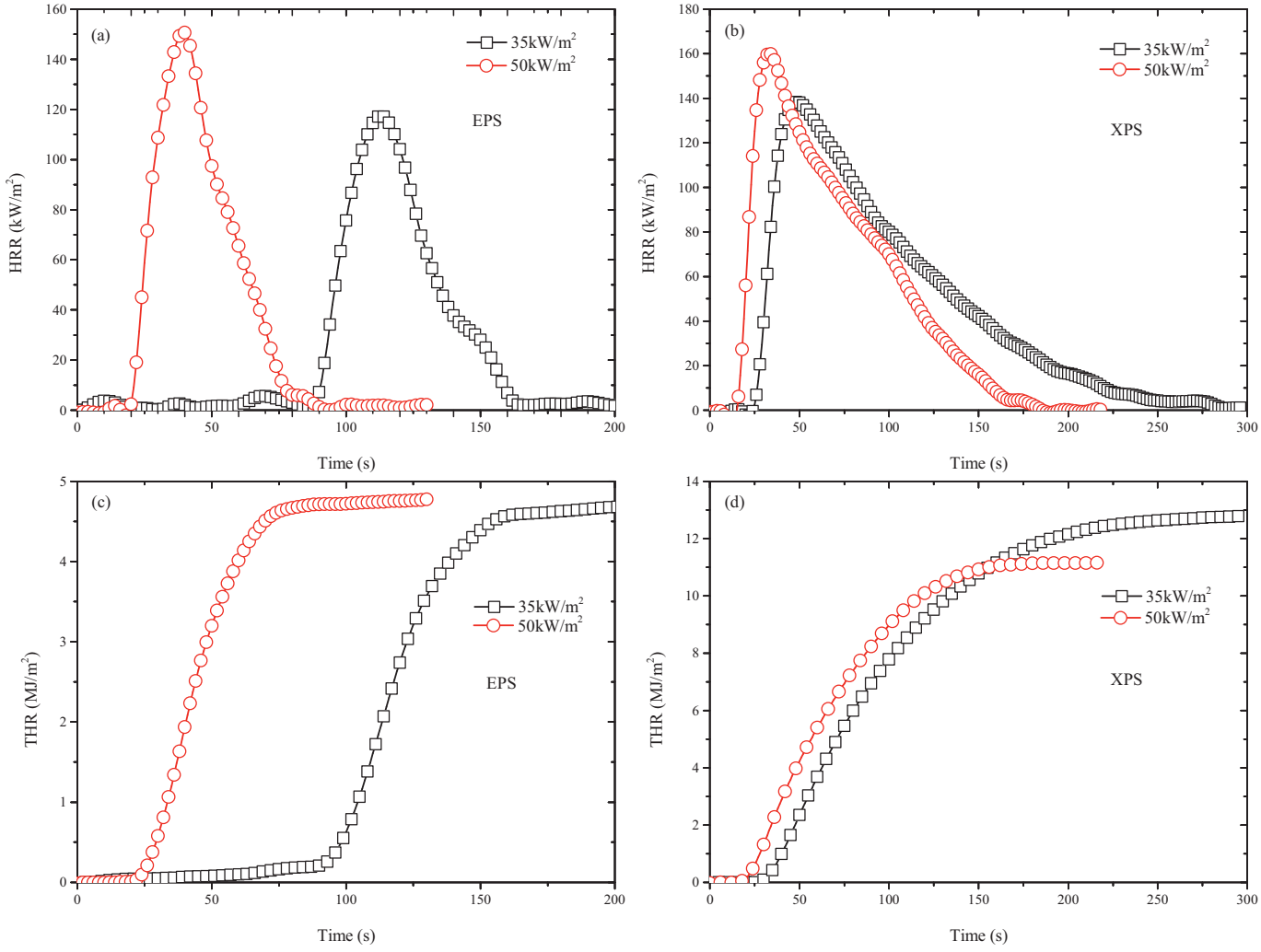

Fig. 6. Cone calorimetric results of EPS and XPS at three heat fluxes.

Table 3
The parameters of cone calorimetry.

Heat flux (kW/m^2)	EPS					XPS				
	TTI (s)	PHRR (kW/m^2)	TTP (s)	FPI (s·kW/m^2)	FGI (kW/m^2·s)	TTI (s)	PHRR (kW/m^2)	TTP (s)	FPI (s·kW/m^2)	FGI (kW/m^2·s)
35	87	117.42	113	0.74	1.04	24	138.32	48	0.17	2.88
50	19	150.69	39	0.13	3.86	15	160.10	33	0.09	4.85

Declaration of competing interest

The authors declare that they have no known conflicts of interest that may affect the work reported in this paper.

Acknowledgement

This study is sponsored by the National Natural Science Foundation of China (No. 51806202), Science and Technology Research Program of the Department of Education in Hubei Province, China (No. B2021001) and Fundamental Research Funds for National Universities, China University of Geosciences (Wuhan).

References

An, W., Jiang, L., Sun, J., Liew, K., 2015. Correlation analysis of sample thickness, heat flux, and cone calorimetry test data of polystyrene foam. J. Therm. Anal. Calorim. 119 (1), 229–238.
Chauhan, R., Gopinath, S., Razdan, P., Delattre, C., Nirmala, G., Natarajan, R., 2008. Thermal decomposition of expanded polystyrene in a pebble bed reactor to get higher liquid fraction yield at low temperatures. Waste Manag. 28, 2140–2145.
Chen, R., Li, Q., Xu, X., Zhang, D., 2019a. Comparative pyrolysis characteristics of representative commercial thermosetting plastic waste in inert and oxygenous atmosphere. Fuel 246, 212–221.
Chen, R., Li, Q., Zhang, Y., Xu, X., Zhang, D., 2019b. Pyrolysis kinetics and mechanism of typical industrial non-Tyre rubber wastes by peak-differentiating analysis and multi kinetics methods. Fuel 235, 1224–1237.
Ding, Y., Ezekoye, O.A., Lu, S., Wang, C., 2016. Thermal degradation of beech wood with thermogravimetry/Fourier transform infrared analysis. Energy Convers. Manag. 120, 370–377.
Ding, Y., Fukumoto, K., Ezekoye, O.A., Lu, S., Wang, C., Li, C., 2020a. Experimental and numerical simulation of multi-component combustion of typical charring material. Combust. Flame 211, 417–429.
Ding, Y., Huang, B., Li, K., Du, W., Lu, K., Zhang, Y., 2020b. Thermal interaction analysis of isolated hemicellulose and cellulose by kinetic parameters during biomass pyrolysis. Energy 195, 117010.
Ding, Z., Liu, J., Chen, H., Huang, S., Evrendilek, F., He, Y., Zheng, L., 2021. Co-pyrolysis performances, synergistic mechanisms, and products of textile dyeing sludge and medical plastic wastes. Sci. Total Environ. 799, 149397.
Faravelli, T., Pinciroli, M., Pisano, F., Bozzano, G., Dente, M., Ranzi, E., 2001. Thermal degradation of polystyrene. J. Anal. Appl. Pyrolysis 60, 103–121.
Flynn, J., Wall, L., 1966. A quick, direct method for the determination of activation energy from thermogravimetric data. J. Polym. Sci., Part B: Polym. Lett. 4, 323–328.
IS0-5660-1, 2002. Reaction-to-fre Tests-heat Release, Smoke Production and Mass Loss Rate —Part 1 Heat Release Rate (Cone Calorimeter Method) Switzerland.
Jian, R., Chen, L., Chen, S.Y., Long, J., Wang, Y., 2014. A novel flame-retardant acrylonitrile-butadiene-styrene system based on aluminum isobutylphosphinate and red phosphorus: flame retardance, thermal degradation and pyrolysis behavior. Polym. Degrad. Stab. 109, 184–193.
Jiang, L., Zhang, D., Li, M., He, J., Gao, Z., Zhou, Y., Sun, J., 2018. Pyrolytic behavior of waste extruded polystyrene and rigid polyurethane by multi kinetics methods and py-GC/MS. Fuel 222, 11–20.
Jiao, L., Sun, J., 2014. A thermal degradation study of insulation materials extruded polystyrene. Procedia Eng. 71, 622–628.
Jiao, L., Xu, G., Wang, Q., Xu, Q., Sun, J., 2012. Kinetics and volatile products of thermal degradation of building insulation materials. Thermochim. Acta 547, 120–125.
Jun, H.C., Oh, S.C., Lee, H.P., Kim, H.T., 2006. A kinetic analysis of the thermal-oxidative decomposition of expandable polystyrene. Korean J. Chem. Eng. 23 (5), 761–766.
Khiari, B., Massoudi, M., Jeguirim, M., 2019. Tunisian tomato waste pyrolysis: thermogravimetry analysis and kinetic study. Environ. Sci. Pollut. Res. 26, 35435–35444.
Kumar, S., Singh, D., 2013. Kinetic model & analysis for pyrolysis of waste polystyrene over laumontite. Int. J. Eng. Res. Sci. Technol. 2, 1–7.
Li, M., Jiang, L., He, J., Sun, J., 2019. Kinetic triplet determination and modified mechanism function construction for thermo-oxidative degradation of waste polyurethane foam using conventional methods and distributed activation energy model method. Energy 175, 1–13.
Li, A., Zhang, W., Zhang, J., Ding, Y., Zhou, R., 2020a. Pyrolysis kinetic properties of thermal insulation waste extruded polystyrene by multiple thermal analysis methods. Materials 13 (24), 5595.
Li, T., Song, F., Zhang, J., Liu, S., Xing, B., Bai, Y., 2020b. Pyrolysis characteristics of soil humic substances using TG-FTIR-MS combined with kinetic models. Sci. Total Environ. 698, 134237.
Liu, J., Zhong, F., Niu, W., Su, J., Gao, Z., Zhang, K., 2019. Effects of heating rate and gas atmosphere on the pyrolysis and combustion characteristics of different crop residues and the kinetics analysis. Energy 175, 320–332.
Mangesh, V., Padmanabhan, S., Tamizhdurai, P., Ramesh, A., 2020. Experimental investigation to identify the type of waste plastic pyrolysis oil suitable for conversion to diesel engine fuel. J. Clean. Prod. 246, 119066.
Masri, T., Ounis, H., Sedira, L., Kaci, A., Benchabane, A., 2018. Characterization of new composite material based on date palm leaflets and expanded polystyrene wastes. Constr. Build. Mater. 164, 410–418.
Mehmood, M.A., Ahmad, M.S., Liu, Q., Liu, C., Tahir, M.H., Aloqbi, A.A., Tarbiah, N.I., Alsufiani, H.M., Gull, M., 2019. Helianthus tuberosus as a promising feedstock for bioenergy and chemicals appraised through pyrolysis, kinetics, and TG-FTIR-MS based study. Energy Convers. Manag. 194, 37–45.
Miura, K., 1995. A new and simple method to estimate f(E) and k0(E) in the distributed activation energy model from three sets of experimental data. Energy Fuel 9 (2), 4–7.
Ni, X., Wu, Z., Zhang, W., Lu, K., Ding, Y., Mao, S., 2020. Energy utilization of building insulation waste expanded polystyrene: pyrolysis kinetic estimation by a new comprehensive method. Polymers 12, 1744.
Nisar, J., Ali, G., Shah, A., Iqbal, M., Khan, R.A., Anwar, F., Ullah, R., Akhter, M.S., 2019. Fuel production from waste polystyrene via pyrolysis: kinetics and products distribution. Waste Manag. 88, 236–247.
Niu, S., Yu, H., Zhao, S., Zhang, X., Li, X., Han, K., Lu, C., Wang, Y., 2018. Apparent kinetic and thermodynamic calculation for thermal degradation of stearic acid and its esterification derivants through thermogravimetric analysis. Renew. Energy 133, 373–381.
Peterson, J.D., Vyazovkin, S., Wight, C.A., 2001. Kinetics of the thermal and thermo-oxidative degradation of polystyrene, polyethylene and poly(propylene). Macromol. Chem. Phys. 202 (6), 775–784.
Qi, Y., Ge, Baoxin, Cao, Q., Xi, F., Shi, X., Si, Y., Wang, X., Gao, B., Yue, Q., Xu, X., 2021. Application of sectionalized single-step reaction approach (SSRA) and distributed activation energy model (DAEM) on the pyrolysis kinetics model of upstream oily sludge: construction procedure and data reproducibility comparison. Sci. Total Environ. 774, 145751.
Sahoo, A., Kumar, S., Kumar, J., Bhaskar, T., 2020. A detailed assessment of pyrolysis kinetics of invasive lignocellulosic biomasses (Prosopis juliflora and Lantana camara) by thermogravimetric analysis. Bioresour. Technol. 319, 124060.
Senum, G., Yang, R., 1977. Rational approximations of the integral of the arrhenius function. J. Therm. Anal. Calorim. 11 (3), 445–447.
Shahbeig, H., Nosrati, M., 2020. Pyrolysis of biological wastes for bioenergy production: thermo-kinetic studies with machine-learning method and py-GC/MS analysis. Fuel 269, 117238.
Shahid, A., Ishfaq, M., Ahmad, M.S., Malik, S., Farooq, M.A., Hui, Z., Batawi, A.H., Shafi, M.E., Aloqbi, A.A., Gull, M., 2019. Bioenergy potential of the residual microalgal biomass produced in city wastewater assessed through pyrolysis, kinetics and thermodynamics study to design algal biorefinery. Bioresour. Technol. 289, 121701.
Siddiqui, M.Z., Park, Y., Kang, Y., Watanabe, A., Kim, S., Kim, Y., 2019. Effective use of aluminum-plastic laminate as a feedstock for catalytic pyrolysis over micro and mesoporous catalysts. J. Clean. Prod. 229, 1093–1101.
Starink, M., 2003. The determination of activation energy from linear heating rate experiments: a comparison of the accuracy of isoconversion methods. Thermochim. Acta 404, 163–176.
Stec, A.A., Hull, T.R., 2011. Assessment of the fire toxicity of building insulation materials. Energy Build. 43, 498–506.
Vyazovkin, S., Burnham, A.K., Favergeon, L., Koga, N., Sbirrazzuoli, N., 2020. ICTAC kinetics committee recommendations for analysis of multi-step kinetics. Thermochim. Acta 689, 178597.
Wang, L., Wang, C., Liu, P., Jing, Z., Ge, X., Jiang, Y., 2018. The flame resistance properties of expandable polystyrene foams coated with a cheap and effective barrier layer. Constr. Build. Mater. 176, 403–414.
Wang, C., Bi, H., Lin, Q., Jiang, X., Jiang, C., 2020. Co-pyrolysis of sewage sludge and rice husk by TG–FTIR–MS: pyrolysis behavior, kinetics, and condensable/non-condensable gases characteristics. Renew. Energy 160, 1048–1066.
Xu, F., Wang, B., Yang, D., Hao, J., Qiao, Y., Tian, Y., 2018. Thermal degradation of typical plastics under high heating rate conditions by TG-FTIR: pyrolysis behaviors and kinetic analysis. Energy Convers. Manag. 171, 1106–1115.
Yu, S., Su, W., Wu, D., Yao, Z., Liu, J., Tang, J., Wu, W., 2019. Thermal treatment of flame retardant plastics: a case study on a waste TV plastic shell sample. Sci. Total Environ. 675, 651–657.
Zhang, W., Zhang, J., Ding, Y., He, Q., Lu, K., Chen, H., 2021. Pyrolysis kinetics and reaction mechanism of expandable polystyrene by multiple kinetics methods. J. Clean. Prod. 285, 125042.
Zhang, W., Zhang, J., Ding, Y., Zhou, R., Mao, S., 2022. The accuracy of multiple methods for estimating the reaction order of representative thermoplastic polymers waste for energy utilization. Energy 239, 122112.
Zhao, B., Liu, Y.T., Zhang, C.Y., Liu, D.Y., Li, F., Liu, Y.Q., 2017. A novel phosphoramidate and its application on cotton fabrics: synthesis, flammability and thermal degradation. J. Anal. Appl. Pyrolysis 125, 109–116.